Modeling Pseudomonas aeruginosa biofilm detachment

Roald Kommedal and Rune Bakke

Faculty of Technology (Porsgrunn)
Department of Environmental Technology

Table of content:

Abstract

The mechanisms and modeling of surface biofilm detachment are evaluated in this study using data from

Pseudomonas aeruginosa experiments and a standard one dimensional mass balance biofilm modeling approach.

The aim of this study is to identify an appropriate expression to model the net surface *Pseudomonas aeruginosa*

biofilm detachment. Measured values of biofilm thickness, biomass concentration, low rate shear stress and

substrate concentrations were used to calibrate detachment models. Most literature models were able to stabilize

the simulated biofilm after parameter estimation, however, few showed good quality of fit. Multi-parameter

models proposed here gave good quality of fit, but estimated uncertainties of the parameter values were high.

Detachment rate expressions which included biofilm biomass failed parameter estimation. Based on sensitivity

analysis, model complexity and residual least square error (quality of fit), it was concluded that both a growth

relation, a lumped parameter describing biofilm size and imposed shear stress, should be included in the overall

surface detachment *Pseudomonas aeruginosa* model.

Key word: *Pseudomonas aeruginosa,* biofilm, detachment

Introduction

Detachment may be defined as the transport of bacterial particles from the attached biofilm phase, to the fluid phase. The reversed detachment process, attachment, may be considered as a separate process, or included in the net detachment rate.

Bryers (1988) identified five different categories of detachment: *erosion, sloughing, human intervention, grazing and abrasion*. While sloughing is often considered as a discontinuous stochastic process, erosion is viewed as continuous, taking place uniformly over the biofilm surface. These processes are the major mechanisms of biomass removal from the biofilm, and therefore the main mechanism to balance biofilm growth, enabling the biofilm thickness to reach a pseudo steady state (Rittman, et al., 1992). In fact, detachment is quite analogous to sludge wasting in suspended growth systems (such as the activated sludge process), at least for the active part of the biofilm near the surface. In this paper, the mechanisms and modeling of surface detachment is discussed, starting with a review of detachment mechanisms.

Causes of biofilm detachment are closely connected to the class of detachment as defined by Bryers (1988). While grazing and human intervention is more or less self-explanatory, abrasion is defined as the loss of biofilm biomass due to collisions between biofilm carriers (Characklis, 1990b). Detachment by abrasion has successfully been exploited to control biofilms in moving bed and biofilm airlift suspension reactors (Tijhuis et al., 1996; Gjaltema et al., 1995; Gjaltema et al., 1997). Sloughing appears as release of large particles due to local rupture of the extra cellular network in deeper parts of biofilms. Sloughing may be triggered by strain forces produced by shear liquid forces at the biofilm surface. At some weak point, the strain force equals the tensile strength of the polymer matrix causing this single point to further weaken, initializing a cascade of ruptures downstream (Ohashi and Harada, 1996; Kwok et.al, 1998). Increased osmotic pressure caused by elevated ion concentration in the void fractions also increase the strain on matrix polymers. This effect may be related to changing growth conditions, especially during increasing substrate concentrations when the local pH may drop significantly due to higher respiration rates. Lysis events will also raise the local ion concentration.

Another influence on matrix strength is the amount and composition of extracellular polymeric substances (EPS) present in the biofilm. Applegate and Bryers (1991) observed (20-40 %) lower detachment rates in an oxygen limited biofilm compared to carbon limited conditions, due to a higher EPS fraction and calcium concentration. The EPS amount present is determined by the EPS turnover rate, governed by production and extracellular enzymatic degradation (hydrolysis). Robinson et al. (1984) and Characklis (1990a) describe a direct relation

between the EPS production rate and the specific cellular growth rate. Degradation of EPS has been related to the presence of extracellular hydrolases, and exploited for dispersion in enumeration methods (Salhani and Uelker-Deffur, 1998). Boyd and Charkrabarty (1995) describe the gene level regulation of EPS and an alginate lyasis in *Pseudomonas aeruginosa* biofilms, suggesting *alg K*, the gene encoding alginate lyasis, to be induced by starvation. A similar effect was observed by Xun et.al (1990). Lee (1992) identified an enzymatic activity that released surface binding proteins to the bulk phase. They later found that this activity was pronounced during endogenous respiration (Lee, et.al, 1996). Thus, in situations of limiting substrate availability EPS concentrations may drop due to lower production during sustained hydrolysis. In the depth of biofilms, substrate limitations often occur as a result of transport limitations, which also reduce transport of excreted enzymes. Thus, an increase of extracellular lyases and hydrolases may occur simultaneously, further reducing the EPS concentration, and increasing the probability of a sloughing event. Regulation of exo-enzyme concentration may also be effected by density dependant intercellular communication by compounds like homoserine lactone (Jones et.al, 1993; McLean et.al, 1997). Detachment may therefore result from population or community regulative mechanisms.

The monomeric composition and divalent cat ion concentrations are highly influential on EPS tensile strength (Turakhia and Characklis, 1989), as is the hydrophobic polymer interactions (Gregory, 1989). The influence of ionic and hydrophobicity effects on biofilm structure and morphology is thoroughly discussed by Christensen and Characklis (1990), but these phenomena are ignored in this discussion of detachment.

Erosion is basically a surface process. Thus it is very likely that the liquid shear force directly cause single cell detachment at the biofilm surface. Trulear and Characklis (1982) first studied the detachment effect of shear force, however later work have not resulted in a general relationship between them (Bakke et.al, 1990; Peyton and Characklis, 1993). Since we are dealing with water liquids, advective flow velocity is the dominant variable controlling shear force. However, the local surface velocity field is not only determined by the bulk flow velocity, but also strongly on the morphology of the biofilm surface. DeBeer and Stoodley (1995) showed that at higher bulk liquid velocities the mass transfer boundary layer, and thus the local velocity field, closely followed the local biofilm surface morphology, while at lower flow rates the velocity field followed the substratum morphology. Not only erosion, but also transport of dissolved substrates is strongly controlled by bulk flow velocity (Lewandowski et.al, 1994). The combined effect of increased local erosion rates and increased substrate transport, and thus higher local growth rate, indicates a local negative feedback regulation of biofilm thickness at varying shear rates. Tijhuis, et.al (1996) argues that biofilm thickness is by large dominated by this interactive

effect of bulk velocity on biofilm erosion and growth rate. Kwok et.al, (1998) also recognize these processes to dominate the morphology and structure of the biofilm.

No:	Model	Reference
1	$r_{det} = k_{det} \cdot L_f$	Peyton and Characklis (1992)
2	$r_{det} = k_{det} \cdot X \cdot L_f$	Bakke et.al (1984); Melo and Bott (1997)
3	$r_{det} = k_{det} \cdot X \cdot L_f^2$	Wanner and Gujer (1986)
4	$r_{det} = k_{det} \cdot L_f^2$	Stewart et.al (1996)
5	$r_{det} = k_{det} \cdot X^2$	Bryers (1987) ; Trulear and Characklis (1982)
6	$r_{det} = k_{det} \cdot \dot{m}_s \cdot L_f$	Speitel and DiGiano (1987)
7	$r_{det} = k_{det} \cdot \dot{m}_s \cdot X \cdot L_f$	Peyton and Characklis (1993)
8	$r_{det} = k_{det} \cdot \dot{m}_s \cdot X \cdot L_f^2$	Stewart (1993)
9	$r_{det} = k_{det,0} \, X \cdot L_f^2 + k_{det,1} \dot{m}_s \cdot X \cdot L_f^2$	Stewart (1993)
10	$r_{det} = k_{det} \cdot \dot{m}_s \cdot L_f + k_{det,0} \cdot L_f$	Speitel and DiGiano (1987)
11	$r_{det} = k_{det} \cdot X \cdot t$	Bakke et.al (1990)
12	$r_{det} = k_{det} \cdot X \cdot t^{0.58}$	Rittmann (1982)
13	$r_{det} = k_{det,0} \cdot \dot{m}_s^{k_{det,1}}$	Tested here
14	$r_{det} = k_{det,0} \cdot L_f^{k_{det,1}}$	Tested here
15	$r_{det} = k_{det,0} \cdot X^{k_{det,1}}$	Tested here
16	$r_{det} = k_{det,0} \cdot (\dot{m}_s \cdot L_f)^{k_{det,1}}$	Tested here
17	$r_{det} = k_{det,0} \cdot (\dot{m}_s \cdot X)^{k_{det,1}}$	Tested here
18	$r_{det} = k_{det,0} \cdot (X \cdot L_f)^{k_{det,1}}$	Tested here
19	$r_{det} = k_{det,0} \cdot \dot{m}_s^{k_{det,1}} \cdot L_f^{k_{det,2}}$	Tested here
20	$r_{det} = k_{det,0} \cdot \dot{m}_s^{k_{det,1}} \cdot X^{k_{det,2}}$	Tested here
21	$r_{det} = k_{det,0} \cdot L_f^{k_{det,1}} \cdot X^{k_{det,2}}$	Tested here
22	$r_{det} = k_{det,0} \cdot \dot{m}_s^{k_{det,1}} \cdot L_f^{k_{det,2}} \cdot X^{k_{det,3}}$	Tested here
23	$r_{det} = k_{det,0} \cdot (\dot{m}_s \cdot L_f)^{k_{det,1}} \cdot t^{k_{det,2}}$	Tested here
24	$r_{det} = k_{det,0} \cdot \dot{m}_s^{k_{det,1}} \cdot L_f^{k_{det,2}} \cdot t^{k_{det,3}}$	Tested here
25	$r_{det} = k_{det,0} \cdot \dot{m}_s^{k_{det,1}} \cdot L_f^{k_{det,2}} \cdot X^{k_{det,3}} \cdot t^{k_{det,4}}$	General model tested here (used during sensitivity analysis)

Table 1. Literature expression used for modeling biofilm detachment, and tested models in this study.

As for sloughing, surface erosion must be considered as being triggered when the shear forces exceeds the adhering force of the individual cell. Again, the adhering force is governed by the amount of EPS, and the composition of the polymers. In addition, surface charge and the resulting hydrophobicity of the bacterial surface cells adds on to the adhering properties. Allison et.al (1990) found that cell hydrophobicity decreased as growth rates where increasing. Also, they found that daughter cells early in their division cycle, had an additional lowered hydrophobicity indicating high dispersal rates during elevated growth rates.

The aim of this paper is to identify an appropriate expression to model the net surface *Pseudomonas aeruginosa* biofilm detachment. Stewart (1993), using a theoretical approach, presents a general mathematical framework for detachment modeling. Several proposed models, including those analyzed by Stewart (1993), are evaluated here using data given by Bakke (1986) and Bakke et al. (2001). Table 1 show typical expressions found in the literature, together with extensions and two general models evaluated in this study. As one may notice, all specific models are variants of the generalized model (no. 25). These are included partly to test literature models, and to compare these qualitatively by the least square fit error residuals. The study is restricted to the following surface related factors: *specific growth rate (*μ*), biofilm thickness (*L_f*), biomass concentration (X) and surface shear stress (*τ*)*.

Modeling approach

The Monod growth expression is the most common growth model for microorganisms. Depending on the substrate concentration, the monod relation is at its maximum a first order process in biomass. During biofilm growth, detachment must be powerful enough to stabilize the biofilm thickness at any growth rate. However, thin biofilms must be allowed to growth without being eroded as a consequence of detachment. Thus, detachment expressions must normally be non-linear in one or several variables, or as a combination of variables.

The general adapted mixed culture biofilm model (MCB) given by Wanner and Guijer (1986) was implemented in the AQUASIM simulation program as a distinguished reactor compartment (Reichert, 1994). In this model the individual particulate concentrations are converted into particle volume fractions. The liquid fraction, also called the biofilm porosity, is given by:

$$\varepsilon_{lf} = 1 - \sum_i \varepsilon_{sf,i}$$

where $\varepsilon_{sf,i}$ is the individual particle volume fraction (wet volume) given by

$$\varepsilon_{sf,i} = \frac{X_i}{\rho_i}$$

where X_i is the particle concentration [g VSS (dw)/m^3 (biofilm wet vol.)] , and ρ_i is the particle density [g VSS (dw)/m^3 (cell wet vol.)]. In the original version of AQUASIM the porosity was assumed constant in time and space. Thus, the liquid fraction growth rate, $r_{\varepsilon lf}$, was direct proportional to the particle growth rate, in order to keep the liquid fraction constant, and given by

$$r_{\varepsilon lf} = \frac{\varepsilon_{lf}}{1 - \varepsilon_{lf}} \sum_i \frac{r_{x,i}}{\rho_{s,i}}$$

where $r_{x,i}$ is the individual particle growth rate. In the new version (ver. 2) an additional term, $r_{\varepsilon lf}^|$, has been added to the liquid fraction growth expression, enabling a freely defined time or spatial dependent volume fraction distribution.

$$r_{\varepsilon lf} = \frac{\varepsilon_{lf}}{1 - \varepsilon_{lf}} \sum_i \frac{r_{x,i}}{\rho_{s,i}} + r_{\varepsilon lf}^|$$

That means that the biomass concentration may vary in the biofilm, and modeling of all biomass dependant detachment rates given in table 1 may be tested.

Another feature of the new version is the possibility of defining both surface and volumetric (i.e. biofilm internal) detachment and attachment rate coefficients. We will not use this feature due to lack of experimental data on internal detachment and attachment rates. It is also important to recognize that these features are only applicable in the diffusive matrix biofilm compartment, another improvement of the latest version (Reichert and Wanner, 1997). For further details of the ver.2D, see Wanner and Reichert (1996).

Materials and Methods

A detailed description of the experimental set up is given by Bakke (1986) and Bakke et al. (2001). A rectangular duct (RD) plug flow reactor was employed with controlled recirculation, securing CSTR conditions and control of shear rate. The reactor was inoculated by 1 ml of *Pseudomonas aeruginosa* pure culture and operated in batch mode until stationary phase. Continuous loading of growth media containing 50 mg glucose/l as organic substrate was then introduced. Near oxygen saturation was secured for the entire experiment by injecting air into the substrate loading pipe, and debubble before entry into the reactor compartment. The pure culture assumption was tested during the experiments. Biomass density was measured by measuring biofilm optical density, relating it to biofilm areal TOC via a standard curve (Bakke, 1986; Bakke et.al, in prep). Biofilm thickness was measured using phase contrast light microscopy as described by Bakke and Olsson (1986).   In order to handle particulate variables in AQUASIM, biomass density had to be converted into volume fraction. These data, measured originally as absorbance, was given as biomass per biofilm area (X_A) in g C/$m^2_{biofilm\ surface}$, and had to be converted to ε_{sf} as

$m^3_{cell\ volume}$/$m^3_{biofilm\ volume}$ (w/w). By assuming a *P. aeruginosa* average cell density (ρ_c) of 200000 g VSS_{cell} (dw)/m^3_{cell} (wet vol.), that is 80% liquid fraction per cell, and an average cellular carbon content (f_{cc}) of 0.53 g C_{cell}/g VSS_{cell} (Christensen and Characklis, 1990), the *P. aeruginosa* volume fraction of the biofilm could be calculated by the following expression:

$$\varepsilon_{sf} = \frac{X_A}{\rho_c \cdot L_f \cdot f_{cc}}$$

where L_f is the measured biofilm thickness. Further, it was assumed that 40 % of the areal biomass concentration was due to EPS. This was measured and confirmed constant through

the experiment (Bakke, 1986).

In order to take into account the measured change in porosity measured by Bakke (1986), a time dependent relaxation expression was chosen for the rate porosity:

$$r^|_{\varepsilon sf} = k_{\varepsilon sf} \cdot (\varepsilon_{sf} - \varepsilon_{sf,final})$$

where $k_{\varepsilon sf}$ is the time dependent relaxation coefficient, and $\varepsilon_{sf,final}$ is the particulate volume fraction at the end of the experiment. $\varepsilon_{sf,final}$ was, based on final stage TEM micro autography (see figure 4), chosen to be 0.55, which is very close to the theoretical particle fraction assuming spherical cells (minimum theoretical porosity is $\pi/6$). The relaxation coefficient was estimated from the measured time dependent biofilm particle fraction using the parameter estimation facility of AQUASIM. Substrate data was equivalently used to estimate the *P. aeruginosa* biofilm growth constants. Finally, measured biofilm thickness time series were used to calibrate each detachment model expression of table 1, by minimizing the sum of squares by the AQUASIM secant algorithm (Reichert, 1998). The effect of low shear rate on the biofilm thickness was also evaluated.

Table 2 lists the state variables, stoichiometric factors and rate processes implemented in Aquasim. Model parameter values are listed in table 3 including literature references and status during the sensitivity analysis. See appendix 1 for details on the *Pseudomonas aeruginosa* model.

	Stoichiometric coefficients "i"				Process rate P_j $[\text{ML}^{-3}\text{T}^{-1}]$
Process	**Dissolved substrate**	**Particulate state variables**			
j	S	X_I	X_S	X_H	
Growth	$-\dfrac{1}{Y_{xs}}$			1	$\mu_{max} \cdot \dfrac{S}{K_S + S} \cdot X_H$
Hydrolysis	$1-f_{X_S}$	f_{X_S}	-1		$k_h \cdot \dfrac{X_S}{K_X} *$
Lysis		f_{Xi}	$1-f_{Xi}$	-1	$k_D \cdot X_H$
	Easily degradable substrate [TOC]	Inert particulate material [TOC]	Slowly biodegradable particulate substrate [TOC]	Biomass [TOC]	Transformation rate: $r_i = \sum_j \boldsymbol{n}_{ji} P_j$ $[\text{M}_i \text{L}^{-3} \text{T}^{-1}]$

Table 2. Process matrix of the *Pseudomonas aeruginosa* model. * Anticipating $X_S \ll X_H$ in the biofilm matrix

Parameter	Value	Sensitivity analysis	Reference
μ_{max}	0.4 1/h	Yes	Characklis (1990a)
K_S	4.0 mg gluc./l	Yes	Characklis (1990a)
$Y_{XS, (max)}$	0.54 g $C_{biomass}$/g $C_{substrate}$	Yes	Characklis (1990a)
k_h	0.12 1/h	No	Henze et.al, (1995)
K_X	0.1 g C_{Xs}/g $C_{biomass}$	No	Henze et.al, (1995)
k_D	0.002 1/h	Yes	Henze et.al, (1995)
f_{Xi}	0	No	Henze et.al (1995)
f_{Xs}	0.1	No	Henze et.al (1995)
ρ_{cell}	0.2 kg (dw)/l (wet vol.)	No	Characklis (1990a)
$D_{glucose}$	$1.25 \cdot 10^{-6}$ m^2/h	Yes	Characklis (1990a)
D_{xs} (Fibrinogen, 350 000 amu)	$1.0 \cdot 10^{-7}$ m^2/h	Yes	Cussler (1984)

Table 3. Parameters used when implemented the process matrix (table 2) in Aquasim. Column three indicates whether or not the parameters were active during sensitivity analysis.

Most are taken from the activated sludge model no. 2 (Henze, et.al, 1995), however the hydrolysis rate expression are changed according to typical biofilm biomass densities (i.e. $X_s << X$), and the decay constant has been lowered due to pure culture conditions (i.e. no predators present) according to the findings of van Loosdrecht and Henze (1998). Diffusion layer thickness was modeled using the model presented by Dawson and Trass (1972):

$$L_B = L_0 \cdot 0.011 \cdot v^{-0.88}$$

where v is the bulk flow velocity (cm/s) and L_0 is the low flow diffusion layer thickness . Initial conditions where as follows: $X_0 = 6$ g/l, $S_0 = 0$ mg/l and $L_{f,0} = 0.2$ μm. For further details regarding definitions and values applied, please refer to appendix 1.

An iterative system identification strategy (figure 1) was used to evaluate the response of modeled biofilm thickness by the detachment models in table 1. a) Linear sensitivity analysis of the general model, b) Parameter estimation of each model to a biofilm thickness time series (Bakke, 1986), c) Simulations of the best fit constant set for presentations of results and d) comparison of models based on quality of fit and model structure (BIC evaluation). Based on BIC value, and relation to proposed a priori detachment mechanisms a *Pseudomonas aeruginosa* pure culture surface detachment model was selected.
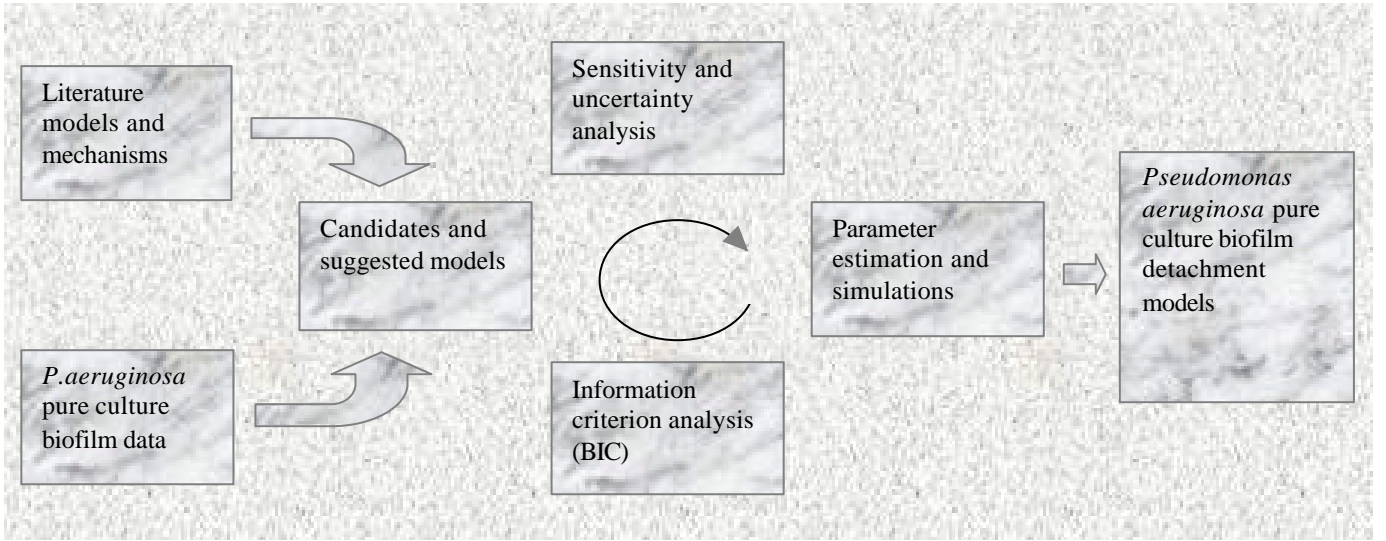
Figure 1 Flow sheet for the iterative system identification process used in this study.

The sensitivity analysis used was the linear response of a state variable, $\delta_{r,p}$ (here biofilm thickness), caused by a 100% change in parameter value. In order to make the sensitivity analysis non-dimensional, a relative sensitivity function was used:

$$\delta_{f,p}^{r,r} = \frac{p}{f}\frac{\partial f}{\partial p}$$

where f is the state variable whose sensitivity to the parameters, p_i is given by $\delta_{r,p}$.

Uncorrelated significant parameters will behave non-symmetrical in the sensitivity plot, with large $\delta_{r,p}$ values. The information criterion discussed by Reichert (1994b) was used in order to give an objective numerical evaluation of the models. The best model has the lowest BIC (B type information criterion) value according to:

$$\text{BIC}\ \left(\mathbf{F}_{\text{meas}}\right) = m \cdot \log(n) - 2 \cdot \log\left[\max_{p}\left(L\left(\mathbf{F}_{\text{meas}},\mathbf{p}\right)\right) \right]$$

where $\mathbf{p}$ is the parameter array, $\mathbf{F}_{\text{meas}}$ is the array of measured data, m is the number of parameters and n the number of data points. L is the weighted least squares likelihood function of the model given by:

13

$$L\left(\mathbf{F}_{meas}, \mathbf{p}\right) = \frac{1}{\sqrt{2\pi}^n} \cdot e^{-\frac{1}{2}\chi^2(\mathbf{p})} \cdot \prod_{i=1}^n \frac{1}{\sigma_{meas,i}}$$

where $\sigma_{meas,i}$ is the standard deviation of $\mathbf{F}_{meas,i}$ and $\chi^2(\mathbf{p})$ is the weighted sum of least squares:

$$\chi^2(\mathbf{p}) = \sum_{i=1}^n \left[\frac{f_{meas,i} - f_i(\mathbf{p})}{\sigma_{meas,i}} \right]^2$$

where $f_{meas,i}$ is the value of data "i" and $f_i(\mathbf{p})$ is the estimated value of data "i". These equations are also used for the *en bloc* parameter estimation routine (Reichert, 1994b).

Assuming uncorrelated parameters in the final parameter set (of the final model), the uncertainty of the simulated state variable (again, here biofilm thickness) may be calculated from the uncertainty of the estimated parameters as:

$$\sigma_f = \sqrt{\sum_{i=1}^m \left(\frac{\partial f}{\partial p_i} \cdot \sigma_{pi} \right)^2}$$

where p_i are the estimated, and thus uncertain, model parameters, and σ_{pi} their estimated standard deviations. Parameter standard deviations are estimated by general linear error propagation from the uncertainty of the data (Reichert, 1994b). Further, the contribution to the total standard deviation of the state variable by the uncertainty of each estimated parameter may be calculated from:

$$\delta_{f,p_i}^{error} = \frac{\partial f}{\partial p_i} \sigma_{pi}$$

This information may be used to identify the major sources of error contribution to the simulated state variable. Even tough this methodology does not consider the non-linear effects of the presented detachment models, it may be used to estimate the order of magnitude of the estimation uncertainty, and it will still identify the major error sources. In addition, it is the only uncertainty analysis available in Aquasim (Monte Carlo simulation is expected to be implemented in the next version (Reichert, 1998b).

Results

Substrate time and space profiles where evaluated in order to establish biofilm properties, and parameter

combinations (growth parameters). Figure 2 shows the least square fit of bulk phase substrate concentration used

to establish the low flow diffusion layer thickness, $L_0 = 12 \ \mu m$.

In order to evaluate the probability of sloughing events, the local biofilm substrate concentrations is plotted in

figure 3. Beyond 200 h it is quite likely that sloughing events would happen, however, significant sloughing

events was not observed, except during shear rate changes (see figure 6). This might be due to EPS carbon

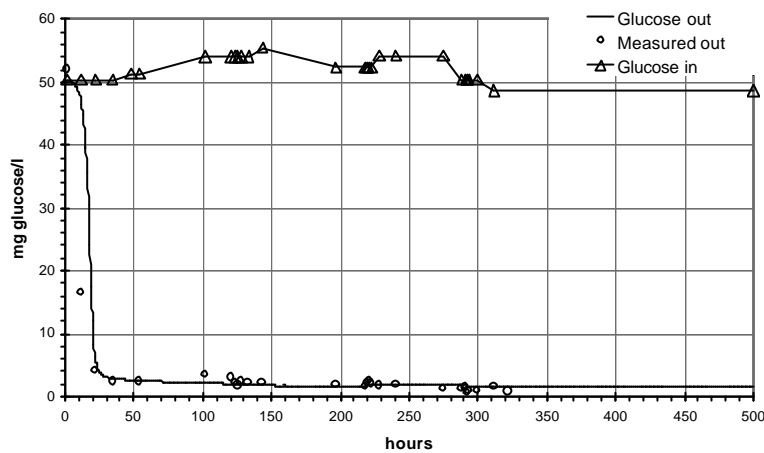recycling which is not incorporated into this model.

Figure 2. Inlet and bulk phase substrate concentrations. Lines are simulated data.
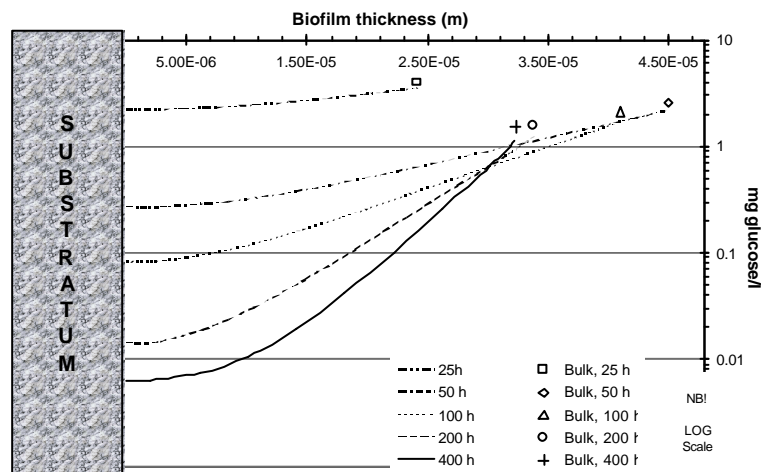

Figure 3. Biofilm substrate concentration profiles at different times. Dots indicate corresponding bulk phase
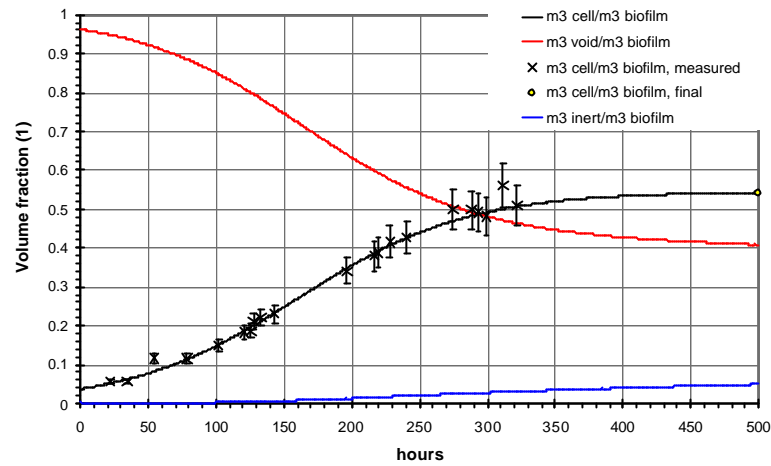   concentrations.

Figure 4. Biofilm biomass (cells + EPS) volumetric fraction development. Final biomass density indicates the theoretical volume fraction occupied by ideal spherical cells.

Figure 4 shows the progression of biomass density, viewed as biomass volume fraction. The biomass relaxation coefficient, k_{esf}, was by least square fit estimation, found to be 0.0298 ± 0.0005 1/h.

Transmission electron microscopy pictures taken at the end of the experiment show the cellular intersect areal density in the biofilm. Figure 5 show a typical biofilm profile from substratum to the biofilm surface, and a close up indicating cellular density near the assumed maximum theoretical volume density of spherical cells.
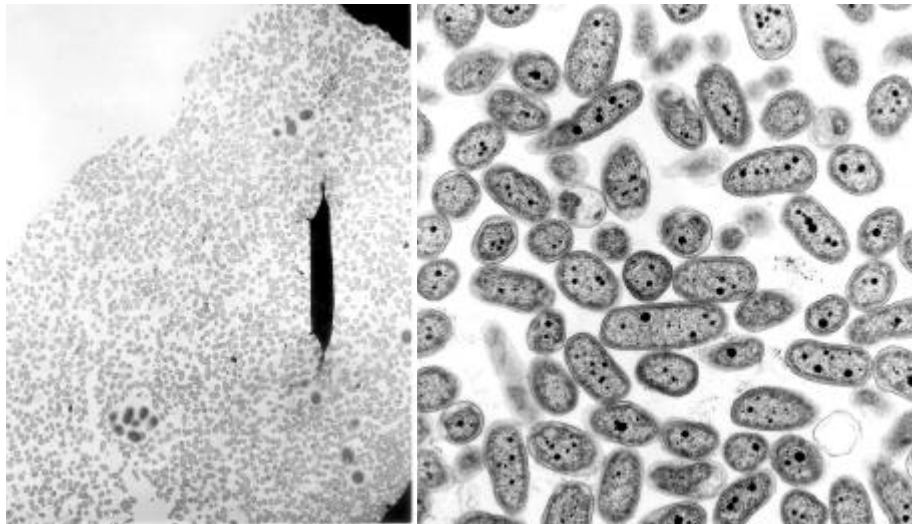

Figure 5. TEM photos of a biofilm transect (left). The biofilm progress from the upper left corner (substratum) to about 35 μm showing a quite uniform volumetric density. A close up (right) indicates the morphology and volumetric density locally in the profile.
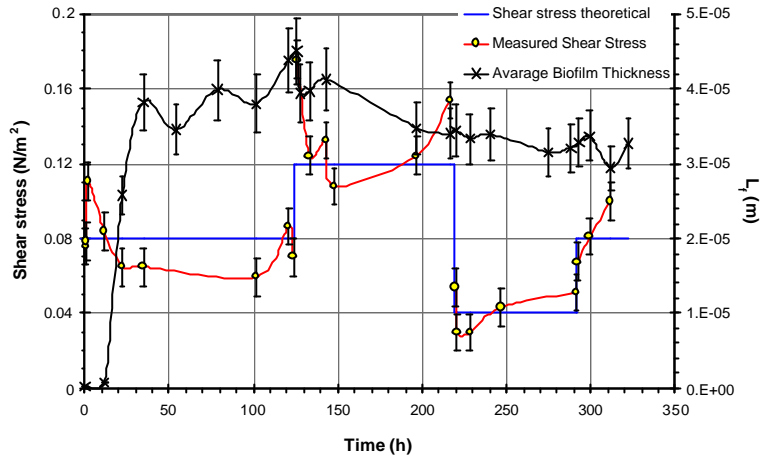
Figure 6. Biofilm thickness at different laminar shear stress. Biofilm thickness error bars indicate standard deviation of eight optical thickness readings, while shear stress readings are assumed to be ± 0.1 N/m^2.

By plotting biofilm thickness progression together with the measured shear stress (figure 6), the direct effect of shear stress of the range 0.04 - 0.12 N/m^2 was assessed graphically. Parameter estimation failed for models which included shear stress and biomass only (i.e. models 11 and 12). However, inclusion of shear stress for the more complex models, improved the quality of fit.

Figure 7 show an identifiability analysis carried out by the sensitivity analysis package implemented in Aquasim (Reichert, 1998). The Aquasim sensitivity algorithm designed for linear sensitivity analysis was used, in absence of a non-linear sensitivity analysis. This algorithm may still give valuable information of model structure,
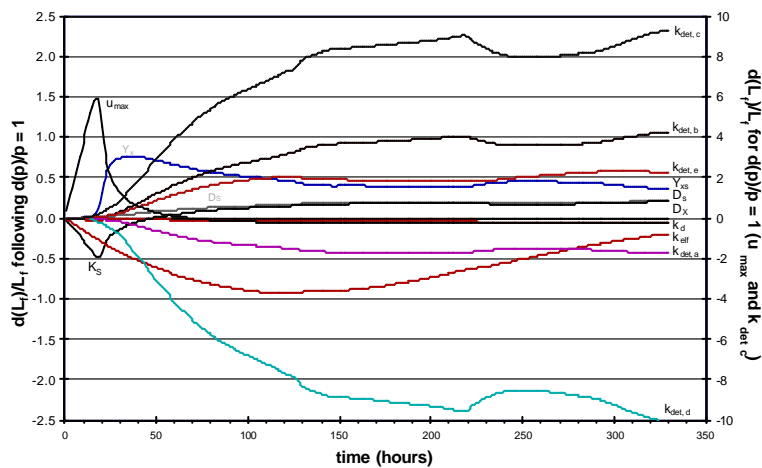

Figure 7. Result of sensitivity analysis using detachment model 25 and key parameters for growth and detachment. The relative change (%) in L_f is given after a 100 % change in parameter value. Note that sensitivity to u_{max} and $k_{det, c}$ refers to the right hand side ordinate.

however, quantitative comparison between the different parameters is not possible (Reichert, 1994). A first order relationship to specific growth rate (μ_S), second order in biofilm thickness (L_f) and half order in biofilm biomass (X) and shear stress (τ) were used.

Table 4 gives the result of parameter estimation of each model listed in table 1. Estimated values, units (when possible) and estimated standard deviations of each parameter is given together with the residual least square error and the resulting BIC value. In cases of estimation failure a manual approach was used (successive simulations and manual comparison of initial χ^2 values). For some models both simulation and parameter estimation failed. In these cases the biofilm thickness either diverged towards infinity, or to zero, indicating a saddle point relationship between the detachment model and biofilm thickness. For some of the non-linear parameter estimations (parameter estimation of models with exponential parameters) the parameter became more and more non-linear (values kept on increasing), compensated by extreme values of the linear detachment coefficient. These values are not likely to have any connection to real detachment mechanisms. In order to terminate parameter estimation, the estimation procedure was therefore manually terminated when no significant improvement in fit resulted from increasing non-linearity (i.e. no significant decrease in χ^2 was observed).

Using the estimated parameters, simulation results for biofilm thickness implementing each model are shown in figure 8 (left: literature models; left: remaining models). Another way of presenting the quality of fit of these models, is to plot the surface biomass concentration (g biomass/m^2 biofilm) time series ($X_A(t) = \varepsilon_{sf}(t) \cdot \rho_s \cdot L_f$). Figure 9 shows this for model 1-10 (left) and 11-25 (right). This plotting combines the detachment model, biomass progression ($\sim k_{elf}[\varepsilon_{sf,final} - \varepsilon_{sf}(t)]$) and growth, and gives an impression of quality of fit for the entire model. The latter plots include the information from the biomass density model (figure 2).

Discussion

Octave Levenspiel, the author of "Omnibook for chemical process engineering" (Levenspiel, 1989) gave this plea for cautiousness in numerical parameter estimation: "given a polynomial model and any comprehensive data set one may obtain perfect fit using four parameters, using five parameters you may draw an elephant and by including a sixth constant one might make the elephant wag the tail." This story illustrates the point of over-parameterization. Complexity of fitted models intrinsically allows high quality fitting, however, it does not necessarily bring you closer to the real mechanisms of the process studied. Thus, simplicity must be a decisive factor in system identification.

no.	Detachment coefficients	St.dev. (estimated)	Units	Final χ^2 value	BIC value	Identifiability
1	$k_{det} = 1.91 \cdot 10^{-2}$	$2.25 \cdot 10^{-3}$	$g/m^4 \cdot h$	1267	783	ok
2	$k_{det} = 6.25 \cdot 10^{-7}$	-	$1/m \cdot h$	4578	4094	Parameter estimation failed. Manual estimated
3	$k_{det} = 1.22 \cdot 10^{-2}$	$3.3 \cdot 10^{-3}$	$1/m^2 \cdot h$	2102	1624	ok
4	$k_{det} = 514$	66	$g/m^5 \cdot h$	526	42	ok
5	$k_{det} = 1.05 \cdot 10^{-16}$	-	m^3/g	-	-	Parameter estimation and simulation failed
6	$k_{det} = 0.17$	0.015	g/m^4	702	218	ok
7	$k_{det} = 2 \cdot 10^{-6}$	-	$1/m$	5173	4689	Parameter estimation failed. Manual estimated
8	$k_{det} = 0.114$	$1 \cdot 10^{-6}$	$1/m^2$	1625	1141	ok
9	$k_{det,0} = 0$ $k_{det,1} = 0.114$	- -	$1/m^2$	1625	1146	ok
10	$k_{det,0} = 0.17$ $k_{det,1} = 0$		g/m^4	702	223	ok
11	-	-	-	-	-	Parameter estimation and simulation failed
12	-	-	-	-	-	Parameter estimation and simulation failed
13	-	-	-	-	-	Parameter estimation and simulation failed
14	$k_{det,0} = 1 \cdot 10^{16}$ $k_{det,1} = 5.00$	- -	- -	126.7	-352	Parameter estimation terminated at listed values
15	-	-	-	-	-	Parameter estimation and simulation failed
16	$k_{det,0} = 1.56 \cdot 10^{10}$ $k_{det,1} = 3.03$	$5.85 \cdot 10^{10}$ 0.36	- -	83.00	-396	ok
17	-	-	-	-	-	Parameter estimation and simulation failed
18	-	-	-	-	-	Parameter estimation and simulation failed
19	$k_{det,0} = 1 \cdot 10^{16}$ $k_{det,1} = 2.49$ $k_{det,2} = 4.45$	- - -	- - -	72.67	-401	Parameter estimation terminated at listed values.
20	-	-	-	-	-	Parameter estimation and simulation failed
21	$k_{det,0} = 1 \cdot 10^{16}$ $k_{det,1} = 4.39$ $k_{det,2} = -0.57$	- - -	- - -	80.5	-393	Parameter estimation terminated at listed values
22	$k_{det,0} = 5.6 \cdot 10^{15}$ $k_{det,1} = 4.61$ $k_{det,2} = 4.58$ $k_{det,3} = 0.57$	- - - -	- - - -	69.53	-399	Parameter estimation terminated at listed values.
23	$k_{det,0} = 5.84 \cdot 10^9$ $k_{det,1} = 3.04$ $k_{det,2} = -0.46$	$2.47 \cdot 10^{10}$ 0.35 0.25	- - -	69.1	-404	ok
24	$k_{det,0} = 1 \cdot 10^{16}$ $k_{det,1} = 2.51$ $k_{det,2} = 4.61$ $k_{det,3} = -0.64$	- - - -	- - - -	56.1	-412	Parameter estimation terminated at listed values.
25	$k_{det,0} = 1 \cdot 10^{16}$ $k_{det,1} = 3.00$ $k_{det,2} = 4.64$ $k_{det,3} = 0.13$ $k_{det,4} = -0.62$	- - - - -	- - - - -	55.95	-407	Parameter estimation terminated at listed values.

Table 4 Parameter estimation and stability evaluation of the proposed models in table 1. In addition χ^2- and BIC values of the parameter estimation are listed. Parameter estimation were stopped in cases of ever increasing exponent parameters without significant improvements of fit, or at a linear detachment coefficient of $10^{\pm 16}$. St. dev. are only available for simulations which converged within the estimation interval (not available for estimations where the final value converged at the limit of a parameter interval).
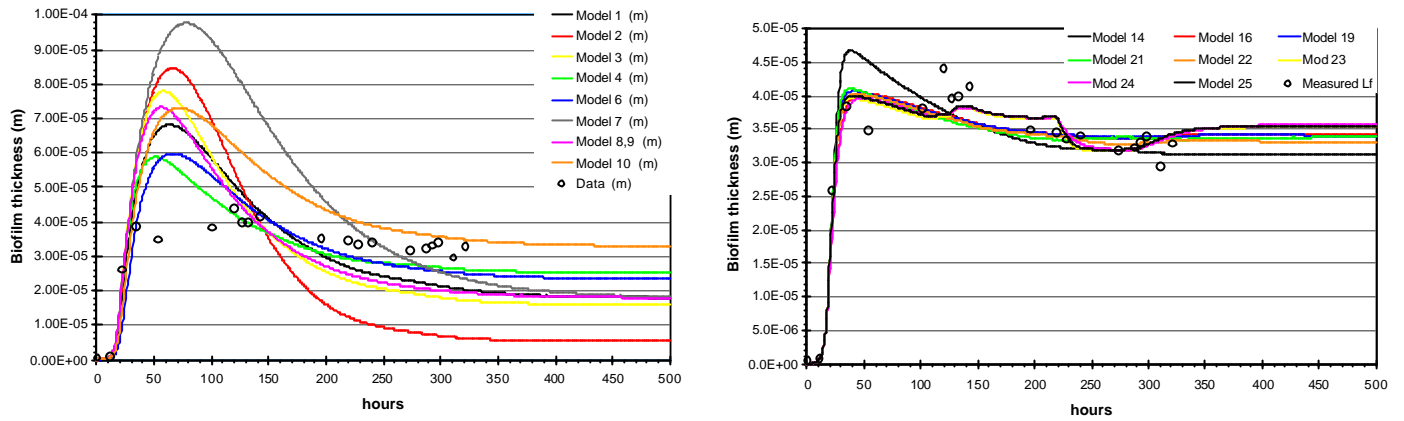
Figure 8 Simulated biofilm thickness using literature models (left) and proposed models listed in table 1. Open circles are measured thickness. Parameters are as listed in table 4.
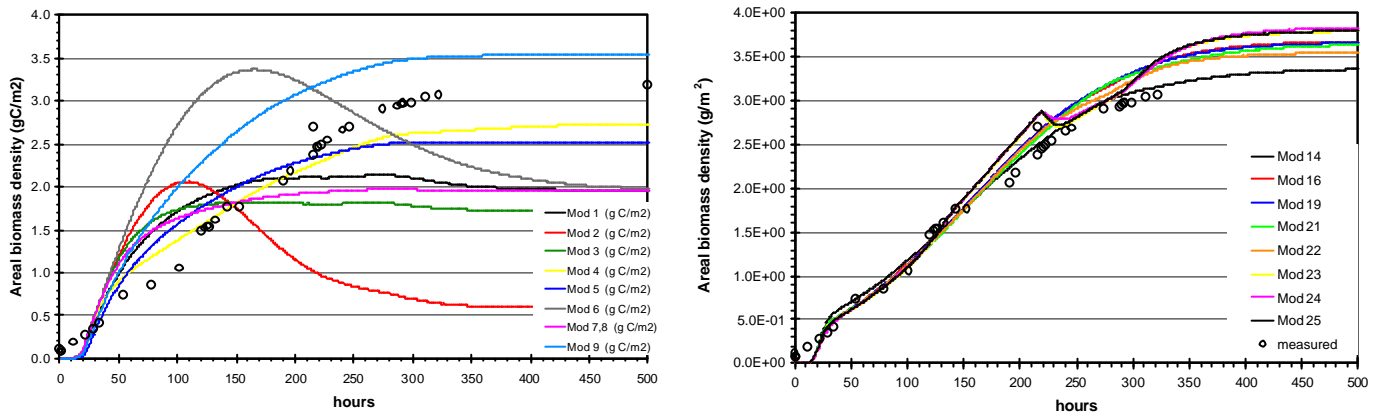

Figure 9 Simulated areal biomass density using the literature models (left) and suggested models listed in table 1. Open circles are measured densities. Parameters are as listed in table 4.

Applying the analysis strategy of figure 1 the first evaluation of the proposed detachment models should be the sensitivity analysis. From figure 7 the first impression is that there seems to be two distinct sets of parameters influencing biofilm thickness significantly. In the early stages growth related parameters (μ_{max}, K_S, and Y_{XS}) are the dominating, while the later stages are more sensitive to biofilm thickness, the linear detachment coefficient, biomass and shear rate. However, the latter parameters show a high degree of linear dependence, suggesting a lumped parameter for aggregated representation. The one showing highest sensitivity should normally represent the best option. An interesting remark here, which also refers to the earlier discussion on the direct detachment effect of shear rate, is that under increasing shear the biofilm thickness shows an expanding response. This may

indicate that the most significant effect of increased shear rate ($8 \rightarrow 12 \rightarrow 4$ N/m^2) under laminar conditions, is the reduction of the boundary layer and not on detachment.

The two phases observed in the sensitivity plot, indicate that the early stages of biofilm progression (thin, and low bacterial densities) are growth controlled, while the medium stages of biofilm development is governed by detachment, and the mature stage is balanced (growth = detachment). This can easily be explained by the density and thickness effect on transport processes. The effect should manifest itself in steeper substrate gradients during the later stages compared to the colonization period, due to limited growth. Figure 10 show the calculated specific growth rate gradients at 20, 30 and 300 hours using model 19. Referring to figure 7 it is clear that indeed the glucose gradients was steeper during the mature phase, and that the substrate concentrations, and thus growth rate, was significantly lower The two, or rally three, phase progression may be directly observed by plotting the simulated difference between growth and detachment (Figure 10, right).
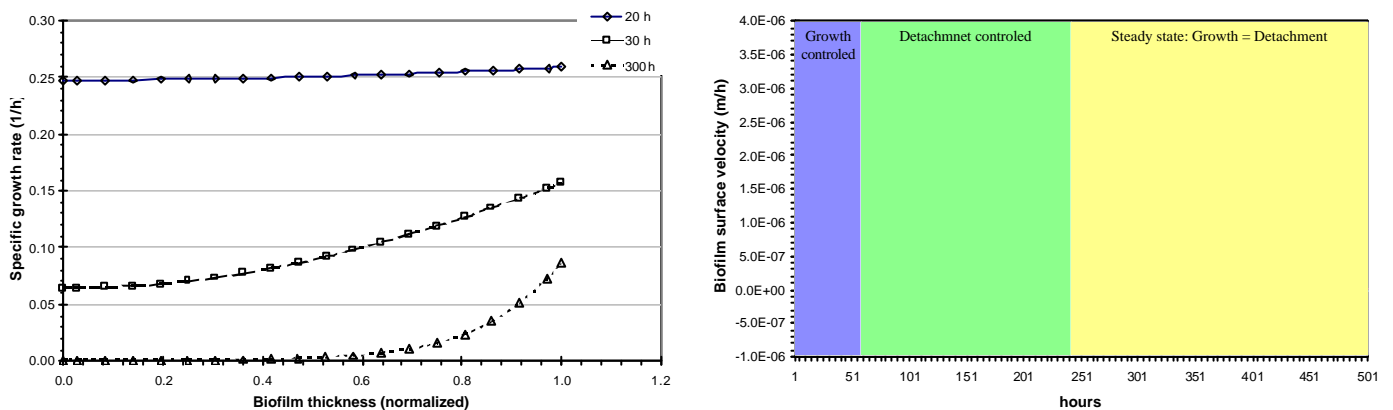

Figure 10 Growth rate gradients into the normalized biofilm at three different phases of the biofilm experiment (left). Growth – Detachment throughout experiment 3 (right), describing three biofilm maturation phases.

So what can be said about the suggested detachment models based on the sensitivity analysis? There seems to be two main conclusions. First, non-linear parameters may be lumped together due to clear linear inter dependence. The most sensitive of these is the biofilm thickness. Second, based on the different forms of the sensitivity curves, a growth relationship seems to be appropriate. K_S, μ_{max} and Y_{XS} show distinct differences (shape) compared to the other parameters for mature biofilm thickness, and maximum specific growth rate is predominant during the growth limited stages. Another interesting effect observed during the sensitivity analysis,

21

was that the standard deviation of the estimated linear detachment parameters was dramatically higher for models that included exponential parameters. Thus, a low degree of non-linearity seems to reduce the overall error of predicting biofilm thickness. Figure 11 show an uncertainty plot of model 4 and model 16. Clearly the implementation of a non-linear parameter increase the uncertainty in L_f prediction, especially due to the uncertainty imposed to the linear detachment coefficient.
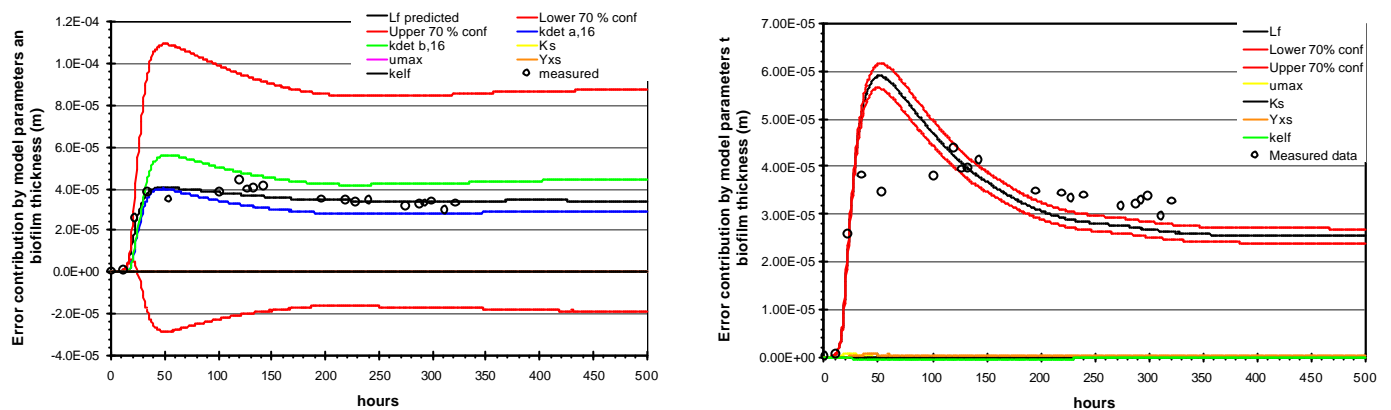

Figure 11 Uncertainty plot of model 16 (left) and model 4 (right). The red line is the predicted biofilm thickness, and the dotted reds indicated the 70 % confidence interval. The other lines present the contribution of each of the growth and detachment related parameters to the error in L_f prediction. The growth related error contributions are of a magnitude of 10^{-3} of the detachment related.

The information criterion used above is one attempt of co-evaluation of models using quality of fit and simplicity. Based on this criteria alone model 24 would be the "best" model. However, the BIC criterion seems to rely very much on χ^2-values, and only to a limited extent complexity has an effect. The decision making process can not be based on such a criteria, however it may at least identify models of no further interest. It seems again appropriate to assess the models from a biological/physiological point of view. In addition, the uncertainty of parameter estimation should also be regarded. Uncertainty plots, such as the one presented in figure 11, should also give information for improving experimental design.

Of the enlisted literature models the model proposed by Speitel and Giano (1987) and Stewart et.al. (1996) showed best fit. A common feature of all models was the problems related to biomass, X. It was not possible to use the Aquasim algorithm for parameter estimation for models including biomass. Also surface related dependencies (i.e. $X_A = XL_f$) failed during parameter estimation, however some models could be assessed using several manual simulations where the parameter value was found by manual comparison to measured biofilm

thickness. For most of these models a typical saddle point effect was observed, where a small increase or decrease of the linear detachment parameter resulted in a divergent biofilm (either fully occupying the reactor, or total vanishing). In addition, the simulated biofilm thickness for all biomass dependant detachment models all had the same shape. This indicates low sensitivity of the biofilm thickness to biofilm biomass concentration. Compared to literature models (where biomass is normally included) and to an intuitive guess based on biological/statistical arguments, this is very surprising. One would think that a dense biofilm would show higher degree of detachment due to the simple fact that the chance of detachment is proportional to the number of cells exposed for the detachment forces. However, higher biomass density also indicates a denser and smoother biofilm with few channels and a regular surface shape. Thus, the higher chance of detachment may be counteracted by less exposure to advective currents, and lower shear forces. Increasing biomass density was observed here (figure 4 and 10), thus the low detachment sensitivity observed may indeed be due to reduced detachment exposure. However, as argued above, this would also reduce substrate penetration into the biofilm resulting in higher probability for a sloughing event, which was not observed in the steady state situations. The effect of biomass influence on detachment should be studied into more detail in order to document a possible direct relationship.

The only detachment model based on a thorough theoretical analysis was given by Stewart (1993), listed in table 1 and 4 as model 8. Compared to model 6, 16 and 19 the only difference is the inclusion of biomass density. χ^2-value indicate that this model is significantly weakened by biomass dependency. This may be due to the fact that Stewart's model is only to be applied for systems of constant biomass (Stewart, 1993). Thus, biomass may be included into the linear detachment constant, resulting in a model closely related to model 16 and 19 which both proved very good quality of fit to our data (omitting X reduce χ^2 from 1625 to 286).

Coming to the tested models proposed in this work, there is a clear tendency of better quality of fit for the more complex models. However, this improved fit is not surprising and moreover, it is even not especially high. Comparing model 16, a rather simple two-parameter non-linear model, to the very complex model 25, only improves the quality of fit by approximately 30%. Therefore, the data presented here are not detailed and comprehensive enough to point in the direction of complex relationships. Figure 12 show graphically the quality of fit when more parameters are included. The major effect of adding an extra parameter, is moving from mono- to a di-parametric
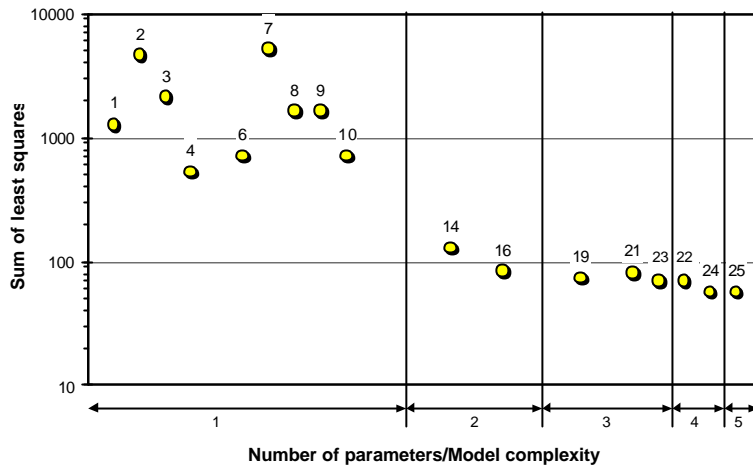
Figure 12 The sum of least squares (χ^2) for the different models as a function of increasing complexity. Indicators refer to model number (see table 1).

models. Also, notice that only non-linear two-parameter models stay di-parametric through the parameter estimation (table 4). Adding more parameters do not significantly improve the quality of fit. That may be due to the similarity of the models, both structural and referring to the variables used. Principal component analysis (PCA) was used to evaluate the similarities of the proposed models of table 1. Figure 13 show PCA results after implementation into the multivariate data analysis program "Unscrambler" (eg. Esbensen *et.al*, 1994).
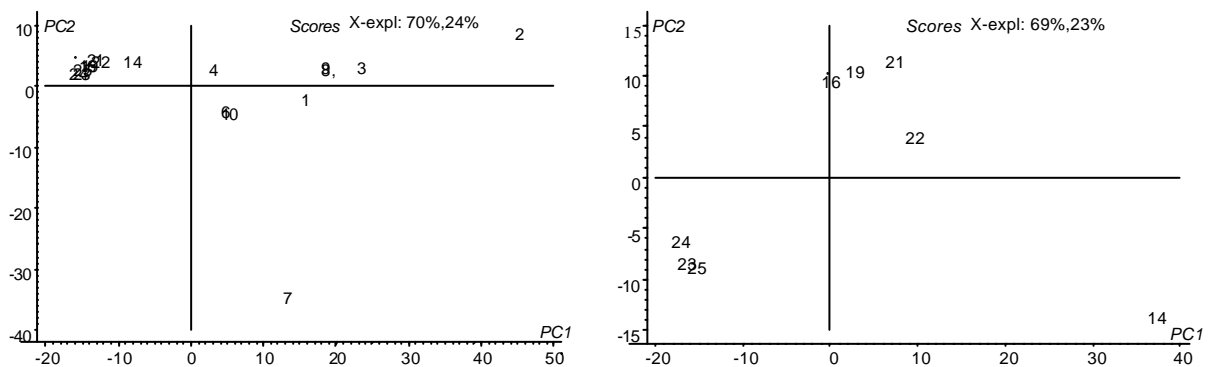

Figure 13 Score plots of PCA analysis of all simulations (left), and reanalysis of models in the non-linear fourth quadrant (right).

PCA score plots show that all the non-linear models are similar compared to the linear ones. From the detailed plot of (figure 13, right) it's quite interesting to see that inclusion of two more parameters into model 23 does not improve the models at all. The major difference between 23, 24 and 25, and the other non-linear models is the inclusion of shear stress. Thus, shear seems to be an important factor for detachment. Model 14 is the non-growth related non-linear model, and show distinct properties. This effect is also seen in figure 8 and 9 where model 14 have exceptionally good fit to the areal biomass density, while producing a poorer fit to the observed biofilm thickness.

The high degree of non-linearity observed for most of the non-linear models are probably due to the fact that the biofilm thickness time series show a rather fast transition from the colonization phase (0-50 h) and the thickness steady state phase. This step-like transition suggests a typical switch function, like the unit step- or Heaviside function, turning on the detachment process to stabilize the thickness expansion. A unit step function may be mimicked by strong non-linearity in a state variable changing at the time of transition. Obviously, the biofilm thickness itself is the best indicator of this point of transition. In order to numerically counter the high power (typically 3-4) of a low number (L_f), the linear detachment constant must be dramatically increased.

Looking at the χ^2 values and the data, comparing them to the relative modest (maybe not for shear rate) transitions made during the execution of experiment 3, one may notice a small effect of the transitions on biofilm thickness. As discussed above, this effect is probably due to the reduction of the mass transfer boundary layer thickness. Therefore it is not surprising that parameter estimation converge at a negative exponential value for shear stress. Detachment may still, however, be directly correlated to shear rate. The effect observed in this experiment is the net effect of growth versus detachment, and therefore, the growth related expansion of the biofilm may here out-value the detachment effect. This illustrates the limitations of this study. Observation of biofilm thickness is the indirect way of observing the growth vs. detachment "battle". Based on a well established growth model and parameter set, it should therefore be possible to extract the detachment information. However, observing biofilm thickness does not produce sufficient accuracy and sensitivity to isolate the details of biofilm detachment by modeling. Simultaneous measurements of bulk phase/effluent biomass concentrations and biofilm thickness would solve this problem.

To sum up the discussion and make recommendations for further studies of biofilm detachment the following proposals should be taken into account:

1. Modeling must relate to the cause of detachment. Thus, the mechanisms (chemical, physical or biological) behind must form the basis of model expression.

2. Experiments must implement strong non-steady state shifts of all relevant state variables in order to produce sufficient sensitivity of the measured effect.

3. Experiments should test a large state intervals in order to test models under dramatically different chemical (growth) and physical (liquid flow) conditions.

4. System identification based on biofilm thickness measurements is not likely to be successful due to possible influence from growth effects, and low sensitivity. Modeling should instead use effluent/bulk phase biomass data directly.

5. System identification should be carried out using a non-linear sensitivity- and parameter estimation algorithm. Implementing the mixed culture biofilm model of Aquasim into MatLab or Maple could solve this.

Conclusion

Literature- and suggested models for net surface detachment rate were fitted to existing data. Measured values of biofilm thickness, biomass concentration, low rate shear stress and substrate concentrations were used to calibrate detachment models. Most literature models were able to stabilize the simulated biofilm after parameter estimation, however, few showed good quality of fit. Multi-parameter models proposed here gave good quality of fit, but estimated uncertainties of the parameter values were high. Detachment rate expressions, which included biofilm biomass, failed parameter estimation, and was therefore not included in the final evaluation. Based on sensitivity analysis, model complexity and residual least square error (quality of fit), it seem to be clear that both a growth relation, a lumped parameter describing biofilm size and the effect imposed by shear stress, should be included in the overall surface detachment *Pseudomonas aeruginosa* model. Of the three qualified models (23, 24 and 25), model 23 must be regarded as the best choice, due to simplicity. However, both models 14 and 16 may be used in shear constant systems, and model 4 is the best choice when uncertainty is to be minimized.

References

Allison, D.G., Evans, D.J., Brown, M.R.W. and Gilbert, P. (1990) Possible involvement of the division cycle in dispersal of *Escherichia coli* from biofilms, Journal of Bacteriology, vol172, no.3, pp. 1667-1669

Applegate, D.H. and Bryers, J.D. (1991) Effects of carbon and oxygen limitations and calcium concentrations on biofilm removal processes, Biotech. Bioeng. vol.37, no.1, pp. 17-25

Bakke, R. (1986) Biofilm detachment, PhD thesis, Montana State University, Bozeman, MT

Bakke, R. and Olsson, P.Q. (1986) Biofilm thickness measurements by light microscopy, Journal of Microbial Methods, vol. 5, pp.93-98

Bakke, R., Characklis, W.G., Turakhia, M.H. and Yeh, A.I. (1990) Modeling a mono-population biofilm system: *Pseudomonas aeruginosa*, in: *Biofilms* (ed: Characklis and Marshall), John Wiley & Sons, New York, 1990

Bakke, R., Kommedal, R. and Kalvenes, S. (2001) Quantification of biofilm accumulation by an optical approach. J. Microb. Meth., 44, pp 13-26.

Bakke, R., Trulear, M.G., Robinson, J.A. and Characklis, W.G. (1984) Activity of *Pseudomonas aeruginosa* in biofilms: Steady state, Biotech. Bioeng., vol.16, pp. 1418-1424

Boyd, A. and Chakrabarty, A.M. (1995) *Pseudomonas aeruginosa* biofilms: Role of the alginate exo-polysaccharide, Journal of Industrial Microbiology, vol.15, pp. 162-168

Bryers, J.D. (1984) Biofilm formation and chemostat dynamics: Pure and mixed culture considerations, Biotech. Bioeng., vol. 26, pp. 948

Bryers, J.D. (1987) Biologically active surfaces: Processes governing the formation and persistence of biofilms, Biotechnology Progress, vol.3, no.2, pp. 57-68

Bryers, J.D. (1988) Modeling biofilm accumulation, in: Physiological models in microbiology (ed.: Bazin, M.J. and Prosser, J.I.), pp. 109-144

Chang, H.T. and Rittmann, B.E. (1987) Biologically active surfaces: Processes governing the formation and persistence of biofilms, Biotecnol. Prog., vol. 3, pp. 57

Chang, H.T. and Rittmann, B.E. (1987) Biologically active surfaces: Processes governing the formation and persistence of biofilms, Biotecnol. Prog., vol. 3, pp. 57

Chang, H.T., Rittmann, B.E., Amar, D., Heim, R., Ehlinger, O. and Lesty, Y. (1991) Biofilm detachment mechanisms in a liquid fluidized bed, Biotech. Bioeng. vol. 38, pp. 499-506

Characklis, W.G. (1990b) Biofilm processes, in: *Biofilms* (ed.: Characklis and Marshall), John Wiley & Sons, New York, 1990

Characklis, W.G., (1990a) Kinetics of microbial transformations, in: *Biofilms* (ed.: Characklis and Marshall), John Wiley & Sons, New York, 1990

Christensen, B.E. and Characklis, W.G., Physical and chemical properties of biofilms, in: *Biofilms* (ed.: Characklis and Marshall), John Wiley & Sons, New York, 1990

Cussler, E.L. Diffusion: Mass transfer in fluid systems, Cambridge University Press, new York 1984

Dawson, D.A., Trass, O. (1972) Mass transfer at rough surfaces, International Journal of Heat and Mass Transfer, vol.15, pp. 1317-1336

de Beer, D. and Stoodley, P. (1995) Relation between the structure of an aerobic biofilm and transport phenomena, Wat. Sci. Tech., vol. 32, no.8, pp 11-18

Esbensen, K., Schönkopf, S. and Midtgaard, T. *Multivariate data analysis in practice: A training package*, Camo AS, 1994

Gjaltema, A., Tijhuis, L., van Loosdrecht, M.C.M. and Heijnen, J.J. (1995) Detachment of biomass from suspended non-growing spherical biofilms in airlift reactors, Biotech. Bioeng., vol. 46, no.2, pp.206-215

Gjaltema, A., van Loosdrecht, M.C.M. and Heijnen, J.J. (1997) Abrasion of suspended biofilm pellets in airlift reactors: Effect of particle size, Biotech. Bioeng., vol. 55, no.1, pp.206-215

Gregory, J. (1989) Fundamentals of flocculation, CRC Critical Review in Environmental Control, vol. 19, no.3, pp. 183-230

Jones, S., Yu, B., Bainton, N.J., Birdsall, M., Bycroft, B.W., Chabra, S.R., Cox, A.J.R., Golby, P., Reeves, P.J., Stephens, S., Winson, M.K., Salmond, G.P.C., Stewart, G.S.A.B. and Williams, P. (1993) The lux autoinducer regulates the production of exo -enzyme virulence determinants in *Erwinia carotovora and Pseudomonas aeruginosa*, EMBO Journal, vol.12, no.6, pp.

Kwok, W.K., Picioreanu, C., Ong, S.L. van Loosdrecht. M.C.M., Ng, W.J. and Heijnen, J.J. (1998) Influence of biomass production and detachment forces on biofilm structure in a biofilm airlift suspension reactor, Biotech. Bioeng., vol. 58, pp.400-407

Lee, S.F. (1992) Identification and characterization of a surface protein-releasing activity in *Streptococcus mutants* and other pathogenic streptococci, Infection and Immunity, vol.60, no.10, pp. 4032-4039

Lee, S.F., Li, Y.H. and Bowden, G.H. (1996) Detachment of *Streptococcus mutants* biofilm cells by an endogenous enzymatic activity, Infection and Immunity, vol.64.no.3, pp. 1035-1038

Levenspiel, O. *The chemical reactor Omnibook,* OSU Bookstores, 1989

Lewandowski, Z., Stoodley, P., Altobelli, S. and Fukushima, E. (1994) Hydrodynamics and kinetics in biofilm systems - Recent advances and new problems, Wat. Sci. Tech., vol. 29, no.10-11, pp.223-229

McLean, R.J.C., Whitley, M., Stickler, D.J. and Fuqua, W.C. (1997) Evidence of autoinducer activity in natural occurring biofilms, FEMS Microbiology Letters, vol. 154, pp. 259-263

Melo, L.F. and Bott, T.R. (1997) Biofouling in water systems, Experimental Thermal and Fluid Science, vol.14, pp. 375-381

Peyton, B.M. and Characklis, W.G. (1992) Kinetics of biofilm detachment, Wat. Sci. Tech., vol.26, no.9-11, pp. 1995-1998

Peyton, B.N, and Characklis, W.G. (1993) A statistical analysis of the effect of substrate utilization and shear stress on the kinetics of biofilm detachment, Biotech. Bioeng. vol. 41, pp. 728-735

Reichert, P. (1994) AQUASIM, a tool for simulation and data analysis of aquatic systems, Water Sci. Tech., vol. 30, pp. 21-30

Reichert, P. (1994b) AQUASIM: Computer program for the identification and simulation of aquatic systems, User Manual, version 1.0, EAWAG, Dubendorf 1994

Reichert, P. (1998) AQUASIM: Computer program for the identification and simulation of aquatic systems, User Manual, version 2.0, EAWAG, Dubendorf 1998

Reichert, P. (1998b) Analysis of transformation of compounds in environmental systems using AQUASIM, PhD course, Technical University of Denmark, spring 1998

Reichert, P. and Wanner, O. (1997) Movement of solids in biofilms: Significance of liquid phase transport, Wat. Sci. Tech., vol. 36, no.1, pp. 321-328

Rittmann, B.E. (1982) The effect of shear stress on biofilm loss rate, Biotech. Bioeng., vol. 24, pp. 501-506

Rittmann, B.E., Trinet, F., Amar, D. and Chang, H.T. (1992) Measurement of the activity of a biofilm: Effects of surface loading and detachment on a three phase liquid fluidized bed reactor, *Wat. Sci. Tech.*, vol.26, no.2-3, pp. 585-594

Robinson, J.A., Trulear, M.G. and Characklis, W.G. (1984) Cellular reproduction and extracellular polymer formation by Pseudomonas aeruginosa in continuous culture. Biotech. Bioeng., vol. 26, pp. 1409-1417.

Salhani, N. and Uelker-Deffur, A. (1998) Improved quantification of aggregated bacteria by combined enzymatic and mechanical treatment of flocs and biofilm from a rotating drum bioreactor, Wat. Res., vol.32, no.4, pp. 1287-1295

Stewart, P.S. (1993) A model of Biofilm Detachment, Biotech. Bioeng., vol. 41, pp. 111-117

Stewart, P.S., Hamilton, M.A., Goldstein, B.R. and Scheider, B.T. (1996) Modeling biocide action against biofilms, Biotech. Bioeng., vol.49, no.4, pp. 445-455

Tijhuis, L., Hijman, B., van Loosdrecht, M.C.M. and Heijnen, J.J. (1996) Influence of detachment, substrate loading and reactor scale on the formation of biofilms in airlift reactors, Appl. Microbiol. Biotechnol., vole 45, no.7, pp7-17

Trulear, M.G. and Characklis, W.G. (1982) Dynamics of biofilm processes, J. Wat. Pol. Control. Fed, vol.54, pp. 1288-1301

Turakhia, M.H. and Characklis, W.G. (1989) Activity of *Pseudomonas aeruginosa* in biofilms: Effect of Calcium, Biotech. Bioeng., vol.33, no. 4, pp. 406-414

Van Loosdrecht, M.C.M. and Henze, M. (1998) Maintenance, endogenous respiration, lysis decay and predation, proceedings of the fourth Kollekolle seminar on Activated Sludge modeling, Copenhagen Denmark

Wanner, O. and Guijer W. (1986) A multi-specie biofilm model, Biotech. Bioeng., vol. 28, pp. 314-328

Wanner, O. and Gujer W. (1986) A multi-specie biofilm model, Biotech. Bioeng., vol. 28, pp. 314-328

Wanner, O. and Reichert, P. (1996) Mathematical modeling of mixed culture biofilms, Biotech. Bioeng., vol. 49, pp. 172-184

Xun, L., Mah, R.A. and Boone, D.R. (1990) Isolation and characterization of disaggregatase from *Methanosarcina mazei* LYC, Appl. and Env. Microbiol., vol. 56, no. 12, pp. 3693-3698